

ELECTRON LENS

V. Previtali

June 28, 2013

1 The electron lens as a collimation device: the idea

The electron lens is a device able generating an electron beam which travels in the same direction of the proton beam. The electron beam shape can be controlled by the shape of the emitting cathode, in order to serve different purposes, i.e. abort gap cleaning, beam-beam compensation and collimation.

In the last years the LHC collimation system has been performing over the expectations, providing the machine with a nearly perfect efficient cleaning system. Nonetheless, when trying to push the existing accelerators to - and over - their design limits, all the accelerator components are required to boost their performances. In particular, in view of the high luminosity frontier for the LHC, the increased intensity would ask for a more efficient cleaning system. In this framework innovative collimation solutions should be evaluated. In this work intends to study the applicability of an hollow electron lens as beam halo scraper for the LHC.

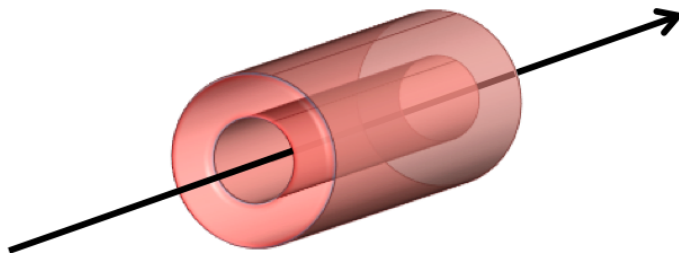


Figure 1: Ideal electron lens distribution.

The hollow electron beam is a device which generates a hollow beam of electrons travelling in the same direction of the proton beam. The de-

scription of the details about the hollow beam generation and technical specifications is not the purpose of this report, and can be found in many past publications [1]. In this work we consider an ideal electron distribution, which consists of a azimuthal-symmetrical distribution of electrons contained between internal radius R_1 and external radius R_2 . The absolute value of R_1 can be arbitrary modified by acting on the solenoidal magnetic field that confines the electron beam, but the ratio $g = R_1/R_2$ is fixed by the geometry of the cathode. For the calculation of the transverse electric and magnetic fields we will approximate the finite-length cylinder with an infinite one, which is legitimate since the transversal space of interest is of the order of few millimeters, while the total device length is typically $L = 2$ m. The fringe fields are neglected.

The electron beam radial profile can be either considered a uniform distribution between R_1 and R_2 (perfect electron lens model), or a more realistic beam profile can be implemented (radial e-lens model model). In both cases the normalized function $f(r)$ does not depend on the angular coordinate and it is defined as:

$$f(r) = I(r)/I_T = \frac{2\pi}{I_T} \int_{R_1}^r r \rho(r) dr \quad (1)$$

where $I(r)$ is the current enclosed in a radius r , I_T is the total electron beam current and $\rho(r)$ is the electron beam density distribution; in the following the function $f(r)$ will be referred as shape function. In case of perfect electron lens the shape is simply:

$$f(r) = \begin{cases} 0 & r < R_1 \\ \frac{r^2 - R_1^2}{R_2^2 - R_1^2} & R_1 < r < R_2 \\ 1 & r > R_2 \end{cases} \quad (2)$$

An example of a measured beam profile, and the fit of a density function $\rho(r)$, are shown in Figure 2.

Thanks to the cylindrical symmetry, the EM field in the space enclosed by the ideal electron beam is perfectly zero, thus not affecting the beam core. On the contrary, protons with transverse radius $r = \sqrt{x^2 + y^2} > R_1$ will feel both the electrostatic force and the Lorentz force for the whole interaction length L . As shown in figure 3, the two forces will sum up when the versus of the proton velocity is opposite to the electron one; otherwise the two forces will have opposite versus.

In our approximation the resulting force can be easily calculated by using the Gauss and the Biot-Savart laws:

$$\vec{F}(r) = \frac{I_r q_p (1 \pm \beta_p \beta_e)}{2\pi \epsilon_0 r v_e} \vec{j}_r \quad (3)$$

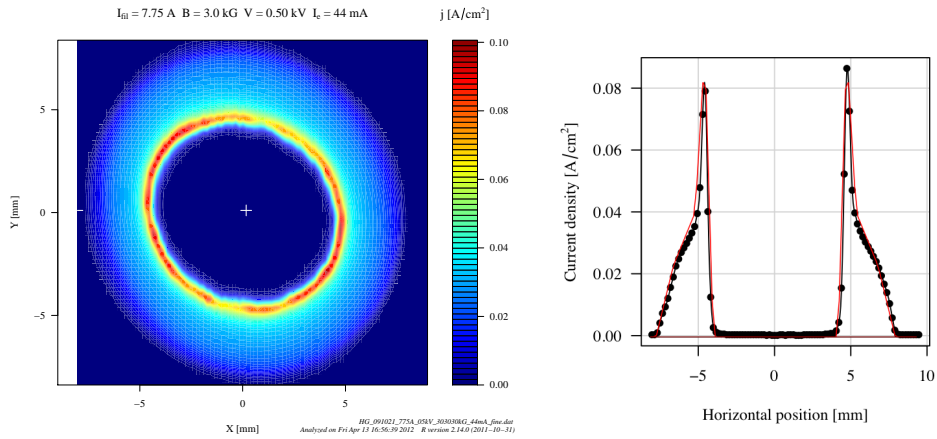


Figure 2: On the left had side, 2D hollow beam measured profiles for a total current of 44 mA, $V=0.5$ KV. On the right hand side the profile in the $y=0$ plane is shown, both experimental data (dotted line) and fit (red curve).

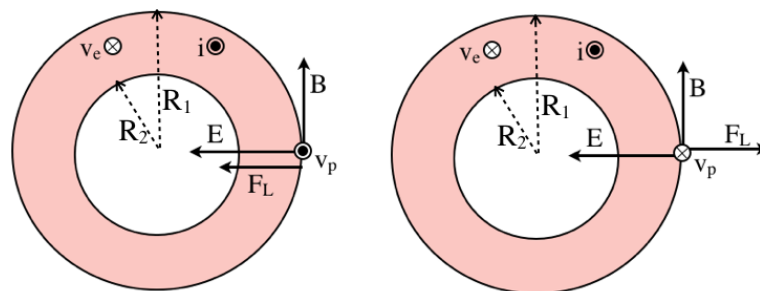


Figure 3: Electrostatic and magnetic force for different proton directions.

where I_r is the current encompassed by the radius r , q_p is the proton charge, β_p and β_e are the relativistic β for the proton and the electron beam, and $\bar{j}_r = (\bar{x} + \bar{y})/r$ is the radial inward direction. Using the definition of shape function $f(r)$ and keeping in mind the definition of angular velocity $\omega = \theta/t = (v_p/r)$, the crossing time $t = L/v_p$, and the centrifugal force $(1/r) = F/(mv_p^2)$, it is possible to calculate the integrated kick for a particle which crosses the electron lens at transverse amplitude r :

$$\theta(r) = \frac{2L f(r) I_T (1 \pm \beta_e \beta_p)}{4\pi\epsilon_0 r (B\rho)_p \beta_e \beta_p c^2} \quad (4)$$

where $(B\rho)_p = m_p v_p / q = 3.3356(mv)_p [GeV/c]$ is the magnetic rigidity of the proton beam.

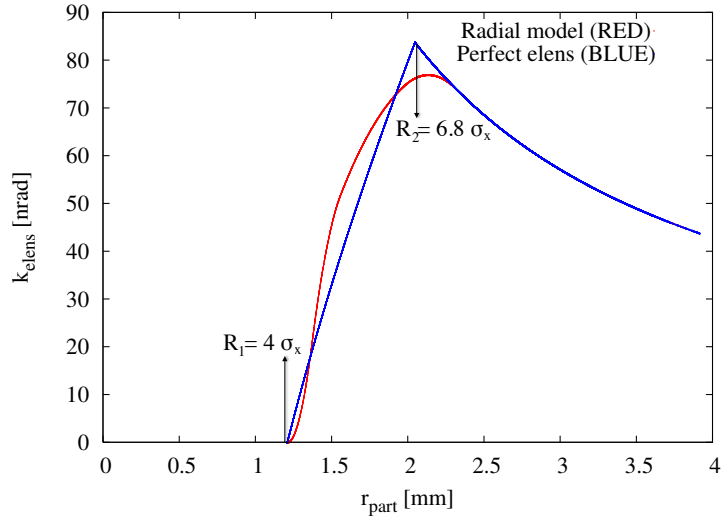


Figure 4: Radial kick given by the electron lens, for both perfect electron lens model and radial profile model.

The typical kick generated by a 1.2 A electron lens on the 7 TeV LHC beam is presented in Figure 4; the details about simulation parameters are described in in Section 2.1). It is interesting to notice how the radial profile provides larger kick in the region between $4.5\sigma_x$ and $6\sigma_x$, but it is less effective for low-amplitude particles. Both models have been implemented in the simulation and tested. Even though preliminary results have been calculated using the perfect electron lens model, the full statistic has been performed only for the radial profile mode. For such reason in this work we present only results from simulations including the radial profile.

Since the electrostatic force is always directed inward, and the electron beam versus is usually chosen such as the Lorentz force adds up to the electric one, the kick given by the electron lens is always directed inwards (focusing), both for the vertical and for the horizontal plane. It follows that, if the kick given by the electron lens is acting constantly on the particle motion (DC mode), the electron lens field becomes a part of the periodic lattice and the single particle invariant for stable particles must be re-defined. The electron lens is therefore expected to introduce a deformation of the phase space together with a positive tune shift of the particle, which would be larger for large particle amplitudes. On the other hand, the DC mode is not the only possible mode of operation of the electron lens: given the extremely fast rising time of the cathode modulator (250 ns) it is possible to modulate the intensity of the electron beam and even to switch it ON-OFF on a turn-by-turn basis. This allows us to use the electron lens both continuously or with a specific modulation. In particular, three different operational modes have been identified:

- DC mode: the electron lens is used in continuous.
- AC mode: the electron lens current is modulated in order to achieve resonance condition with the particle betatron oscillation.
- “white noise” mode: the electron lens is randomly switched on or off in order to steadily heat the beam.

In the next chapters the details of the different operation modes and the effect on the LHC beam as predicted by simulations for the LHC case will be presented.

2 LHC simulations

2.1 Simulation parameters

For a future installation of the electron lens the LHC two possible locations, immediately downstream and upstream of IP4 (RB44-RB46). In this location there are about 420 mm in between the two beam pipes. At first the possibility to insert an already available device (currently in FNAL) has been evaluated, so the outer physical dimensions of such a device has been considered for preliminary implementation studies. Since on the outer side of the ring the QRL (Quench Recovery Line) pipes are very close to the beam pipe, not enough lateral space would have been available for positioning the device for Beam 2. However, thanks to the effort to FNAL engineers and of the LHC integration teams, it was been verified that a simple rotation of the external cryostat of only 10 degrees would have been enough to allow the installation of the device in RB46 for Beam 1. Dispersion is almost totally

LHC- IP4 BEAM 1

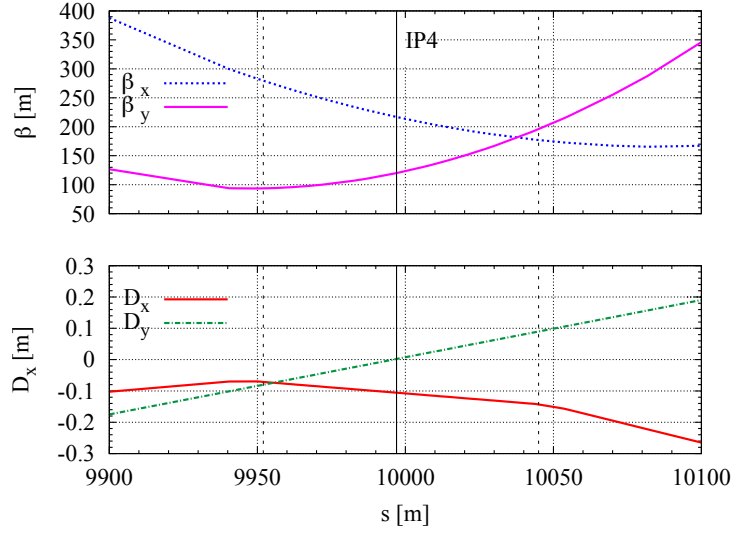


Figure 5: Beta and dispersion functions for the horizontal and vertical orientation at the LSS4, LHC, collision optics for Beam 1.

LHC- IP4 BEAM 2

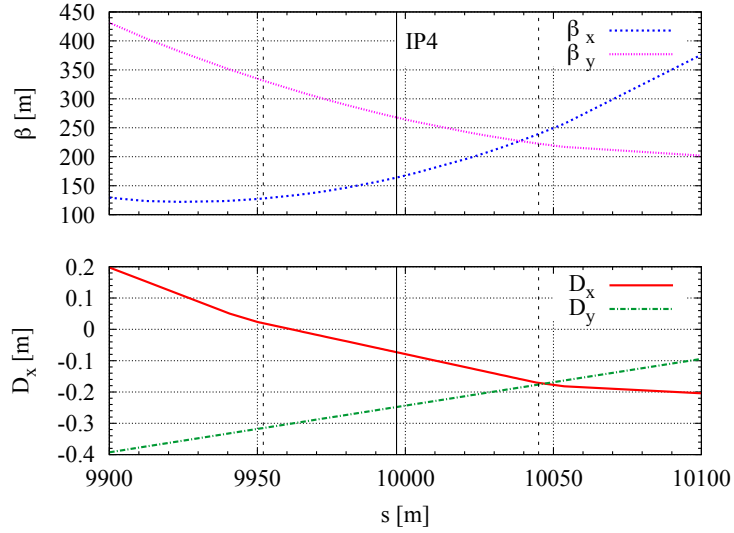


Figure 6: Beta and dispersion functions for the horizontal and vertical orientation at the LSS4, LHC, collision optics for Beam 2.

suppressed in the whole region: it is of the order of 10 cm both in horizontal and in vertical plane. See Figure 5 and Figure 6 for computed optical

function plots (by MADX), both for Beam 1 and Beam 2. Since in RB46 the β -functions are close to round beam both for Beam 1 and for Beam 2, we selected this location for our simulation campaign.

All the simulations assume typical parameters for the electron lens (current 1.2 A, extraction voltage 5 KeV). The nominal 7 TeV LHC squeezed optics has been simulated, sextupoles included, octupoles switched off. The case of purely horizontal (and vertical) halo has been studied, generating an on momentum halo with nominal normalized beam emittance of $3.75 \cdot 10^{-6}$ m rad. Since the results do not substantially differ for the vertical and horizontal case, only the horizontal case is presented in this report. The machine is in storage mode, and no diffusive effects or beam beam interactions have been included. The simulation have been performed with SixTrack (collimation version), where a model describing the ideal electron lens has been implemented as a new collimator-type element.

The inner radius of the electron lens has been fixed to $4\sigma_{x|y}$ in case, respectively, of horizontal or vertical halo simulations. The absolute kick value given by the electron lens in function of the distance from the center is shown in Figure 4, both the simulation results and the analytical expectation.

Table 1: Main optics parameters for the collimators simulated in Sixtrack.

name	s [m]	α_x [-]	β_x [m]	α_y [-]	β_y [m]	μ_x [-]	μ_y [-]
ELENSE	10037	0.318	181.8	-0.962	179.9	24.36	22.24
TCP.D6L7.B1	19789.2	2.120	158.9	-1.097	78.26	47.34	43.42
TCP.C6L7.B1	19791.2	2.051	150.5	-1.153	82.76	47.34	43.42
	σ_x [μ m]	σ'_x [μ rad]	σ_y [μ m]	σ'_y [μ rad]			
ELENSE	302.3	1.74	300.7	2.32			
TCP.D6L7.B1	282.54	4.17	198.3	3.76			
TCP.C6L7.B1	275.02	4.17	203.9	3.76			

2.2 DC mode

As discussed in Section 1, we expect the DC mode of the electron lens to introduce a deformation of the particle orbit in the phase space and a tune shift. This has been verified by simulations.

In case of quasi-linear machine (linear machine and sextupoles), the tune shift of the particle is of the order of few 10^{-4} and depends on particles

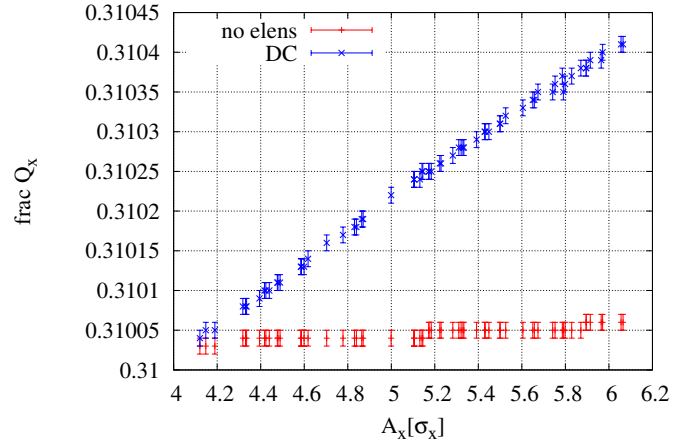


Figure 7: The fractional part of the horizontal tune in dependence on the particle average amplitude for a quasi-linear machine. In case of no electron lens, the slope is caused by the other non linear elements (sextupole) in the optics.

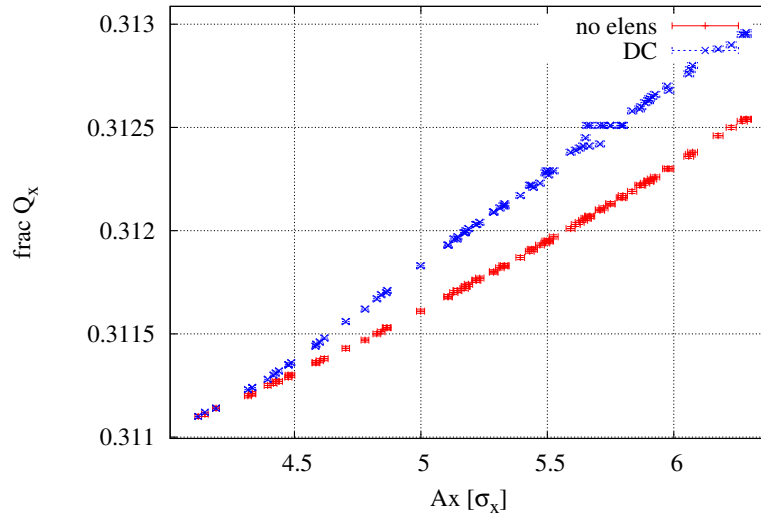


Figure 8: The fractional part of the horizontal tune in dependence on the particle average amplitude, when octupoles are included in the simulation.

initial conditions, as shown in Figure 7: as expected the tune shift is always positive (because the electron lens is always focusing) and larger for particles with a larger betatronic amplitude. Since the electron lens kick amplitude depends linearly on the particle position, it follows that the dependency on the tune shift by the initial amplitude is also linear with the particle initial amplitude. The tune shift reaches a maximum value of about $5 \cdot 10^{-4}$. Given the LHC extremely stable working point, such a tune shift is not sufficient for driving the particle into a high order machine resonance. The jitter in time of the tune is also negligible, at least up to a precision of about $1 \cdot 10^{-5}$.

When including non linear elements such as the octupoles in the simulation, the particle tune is heavily affected: the whole tune range is shifted and the spread is about a factor 100 larger. By dedicate studies it was observed that the regular tune increase with respect to the particle amplitude is interrupted only at about $5.7 \sigma_x$. After further investigation, studying the phase space portraits of particles with about $5.7 \sigma_x$, it was found out that a high-order resonance sits there when the electron lens is present.

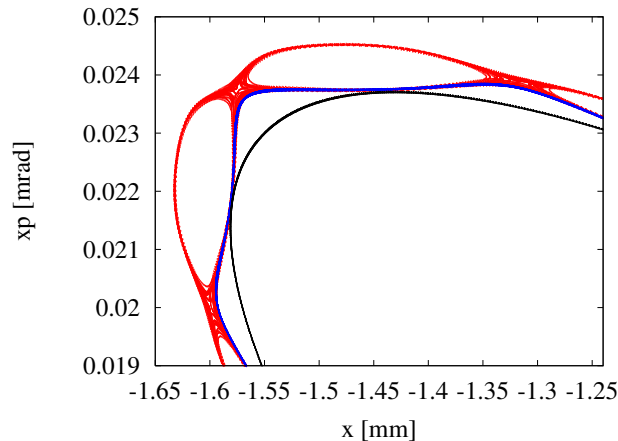


Figure 9: Close-in of the horizontal phase space for the same particle in case with (BLUE) and without electron lens (BLACK), for a particle which has a normalized amplitude of about $5.7 \sigma_x$. The RED line correspond to the case of electron lens with current jitter.

In Figure 9, the deformation of the phase space induced by the non linearity of the electron lens is presented for the electron lens in the non linear machine. A maximum amplitude oscillation of the order of few hundreds of sigma is introduced by the electron lens. When adding a jitter of $\pm 2\%$ in the electron beam current, the electron lens begins to show a diffusive effect, as shown in Figure 9: in this case the amplitude change is enough to drive the particle in the high resonance sitting at about 5.7 sigma.

2.3 AC mode

In order to enhance the efficiency of the electron lens as a scraper, it was proposed to put the electron lens in resonance with the betatronic oscillation of the particles. The basic idea is to use the electron lens for giving a periodic kick which follows the periodicity of the betatronic tune. In order to find the right resonance frequency, it is useful to consider the equation of a purely horizontal (or vertical) motion of a particle at the electron lens location. Neglecting the non linear elements in the machine it is clear that, when the electron lens is not active, the equation of motion in the normalized coordinate space is the equation of an harmonic oscillator:

$$m\ddot{x} + kx = 0 \quad (5)$$

where the natural oscillation frequency $\omega_0 = \sqrt{k/m}$ is the particle betatron tune in the considered plane. When the particle is subject to the electron lens force, the equation becomes:

$$m\ddot{x} + kx = -f(x) \quad (6)$$

where in general $-f(x)$ is an highly non linear force. It is possible however to consider the simple case of a non-hollow flat lens and to study the motion for a limited transverse range, which is a good approximation because the available aperture is limited by the collimator aperture, which is usually lower than the electron lens outer radius. In this case the electron lens the force is nearly linear with the transverse position, and the equation of motion is:

$$\begin{aligned} m\ddot{x} + kx &= -k_{DC} x \\ m\ddot{x} + (k + k_{DC})x &= 0 \end{aligned} \quad (7)$$

and the electron lens effect is simply to increase the particle oscillation frequency from ω_0 to $\omega_{DC} = \sqrt{(k + k_{DC})/m}$. For focusing forces, i.e. $k_{DC} > 0$, the frequency of the oscillation increases (i.e. increases the tune).

We shall now consider the case where the electron lens beam current is variable in time, so that $f = f(x, t)$. Being the e-lens force directly proportional to the total e-beam current, we can decouple the spatial and time-dependent part. A positive modulation function $g(t)$, varying between zero and one, represents the e-lens pulsing waveform; it is natural to start with the simplest possible shape for such function, i.e. a pure harmonic with frequency ω_r :

$$g(t) = (1 + \sin \omega_e t)/2 \quad (8)$$

When the electron lens is modulated, the particle motion equation is therefore:

$$m\ddot{x} + [k + k_{DC}(1 + \sin \omega_e t)] x = 0$$

$$\ddot{x} + \left[\omega_{DC}^2 \left(1 + \frac{k_{DC}}{k + k_{DC}} \sin \omega_e t \right) \right] x = 0 \quad (9)$$

Equation 9 is known, in physics mathematics, as Mathieus equation. In case $\frac{k_{DC}}{k+k_{DC}} \ll 1$, it describes a parametric resonance which is peaked in $\omega_e = 2\omega_{DC} + \epsilon$, with ϵ :

$$-\frac{1}{2} \frac{k_{DC}}{k + k_{DC}} \omega < \epsilon < \frac{1}{2} \frac{k_{DC}}{k + k_{DC}} \omega \quad (10)$$

Considering therelation between the relat on between k and w :

$$k + k_{DC} = w_{DC}^2 m \quad (11)$$

$$k = w_0^2 m \quad (12)$$

and therefore:

$$\frac{k_{DC}}{k + k_{DC}} = \frac{\omega_{DC}^2 - \omega_0^2}{\omega_{DC}^2} \quad (13)$$

Considering the fact that tune and frequency are directly proportional and using the tune values presented in Figure ??, we have that $\omega_{DC} = \omega_0 + \delta\omega$ with $\delta\omega \ll \omega$. The previous equation then is:

$$\frac{k_{DC}}{k + k_{DC}} = \frac{2\omega_0\delta\omega + \delta\omega^2}{\omega_0^2 + 2\omega_0\delta\omega + \delta\omega^2} \approx \frac{2\delta\omega}{\omega_0} \ll 1 \quad (14)$$

which demonstrate that the electron lens case can actually be considered a case of parametric resonance. The parametric resonance width ϵ therefore results:

$$-\delta\omega < \epsilon < \delta\omega \quad (15)$$

meaning that the resonance is excited only if the difference between the applied frequency ω_e and the exact resonance frequency $2\omega_r$ is less than the induced tune spread.

The exact transposition to the case of the non-linear force generated by an hollow electron lens (Figure 4) is not straightforward. Instead of the well-know equation 7, the equation of motion would be:

$$m\ddot{x} + kx = -f(x) \quad (16)$$

where $f(x)$ could be approximated with a high order polynomial. The solution of such a differential equation is not straightforward. In order to identify the optimal excitation frequency, we simulated the scraping effect of an el-lens driven by different multiples of the natural frequency $n \cdot \omega_0$, with the multiplying factor n in the range $\{1, 2...10\}$. However, when octupoles are present, it is difficult to define the natural frequency ω_0 : as shown in

Figure 8 ω_0 spans in a wide range. In order to overcome this complication, the e-lens excitation frequency is varied between $n \cdot 0.3104$ and $n \cdot 0.3136$, in frequency steps of $2 \cdot 10^{-5}$, one step every 10^3 turns. The total number of turns simulated is $2 \cdot 10^5$.

Since the purpose of this simulation is to evaluate the efficiency of the electron lens and not to study the losses in the machine, the simulated collimation system has been reduced to only two elements: an e-lens in AC mode (inner radius $4 \sigma_x$) and a standard LHC horizontal primary collimator in IP7 (TCP.C6L7.B1, aperture $6.2 \sigma_x$). The radial electron lens has been used, and there is no jitter of the electron beam intensity. The primary collimator has been treated as a black absorber. The initial distribution is a uniform flat distribution between 4 and $6 \sigma_x$. The LHC optics is the standard LHC case at 7 TeV with octupoles at maximum strength.

In order to qualify the efficacy of the electron lens as a scraper, we use the global scraping efficiency, defined as:

$$\eta_g(t) = N(t)/N_0 \quad (17)$$

where $N(t)$ is the number of particles which have not been removed after t turns over the initial number of particles N_0 . This quantity is obviously dependent on the initial distribution: for all the simulation presented in this report the initial halo distribution is a uniform flat distribution in the amplitude space between 4σ and 6σ . Only the simulations about horizontal plane are here presented, but the vertical plane presents no significant differences.

In Figure 10 the global scraping efficiency $\rho_s(2 \cdot 10^5)$ is presented for different multiplication factors. It can be noticed that there is a different response to odd and even multiplication factors. The most effective resonance frequency is $2\omega_0$, as expected in the case of simple parametric oscillations.

2.3.1 Optimization of frequency sweep

The electron lens simulated configurations can be divided in two groups: the "low step" series, corresponding to tune step of $2 \cdot 10^{-5}$ and the "high step" series, with tune step of $5 \cdot 10^{-5}$. The total covered range varies from $8 \cdot 10^{-4}$ to $32 \cdot 10^{-4}$ in tune units. Considering the revolution frequency of the LHC $f = 11.245$ KHz, the tune range and the e-lens frequency multiplication factor of two, this is equivalent to sweeping through in the frequency range [43 : 947 : 44.230] KHz with steps of 2.82 Hz (low step case) or 7.06 Hz (high step case) every 89 ms (1000 turns).

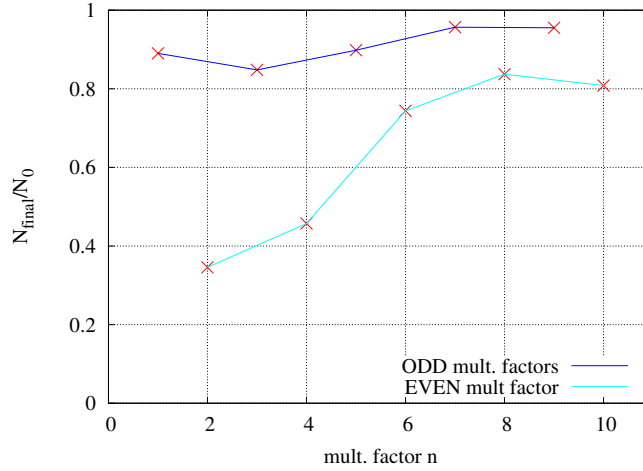


Figure 10: Relative number of survival particles after $2 \cdot 10^5$ turns for different excitation frequency $n \cdot \omega_0$ of the AC electron lens.

Table 2: sweeping parameters

Label	f_{min}	f_{max}	F_{avg}	Δf	Frequency Step	Turns per step
L8	.3116	.3124	.3120	.0008	$2 \cdot 10^{-5}$	10^3
L10	.3115	.3125	.3120	.0010	$2 \cdot 10^{-5}$	10^3
L16	.3112	.3128	.3120	.0016	$2 \cdot 10^{-5}$	10^3
L20	.3110	.3130	.3120	.0020	$2 \cdot 10^{-5}$	10^3
L32	.3104	.3136	.3120	.0032	$2 \cdot 10^{-5}$	10^3
H5	.31175	.31225	.3120	.005	$5 \cdot 10^{-5}$	10^3
H10	.3115	.3125	.3120	.0010	$5 \cdot 10^{-5}$	10^3
H15	.31125	.31275	.3120	.0015	$5 \cdot 10^{-5}$	10^3
H20	.3110	.3130	.3120	.0020	$5 \cdot 10^{-5}$	10^3
H30	.3105	.3135	.3120	.0030	$5 \cdot 10^{-5}$	10^3

A summary table of the tested range-step combinations is presented in Table 2. The corresponding global scraping inefficiencies are presented in Figure 11. Most cases do not significantly differ in global scraping efficiency, as far as the sweeping range is not too different from the tune range we want to cover. In fact we noticed that an optimal sweeping range is between one third and one half of the total tune range.

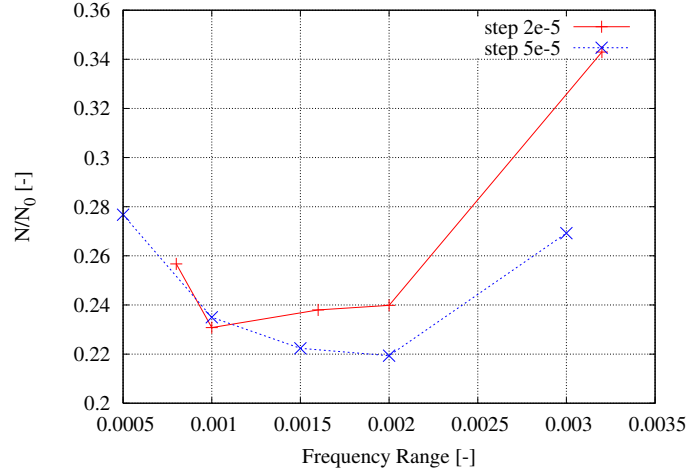


Figure 11: Global inefficiency versus total range scanned, for different steps in frequency.

To study the amplitude distribution of the survival particles, a new qualifying parameter has been introduced, i.e. the local scraping inefficiency $\eta(a, t)$:

$$\eta(a, t) = dN(a, t)/dN_0(a) \quad (18)$$

where $dN(a, t)$ is the number of particles with amplitude in the range $[a, a + da]$ at the turn t and $dN_0(a)$ is the correspondent number of particle at the initial turn. Being a normalized quantity, the local scraping inefficiency has the clear advantage of non depending on the initial distribution.

The local scraping efficiency for the most performing case (i.e. H20) is shown in Figure 12 . It can be noticed that the e-lens is much more effective for high amplitude particles (after about $4.5 \sigma_x$), where the scraping inefficiency is lower than 10^{-2} - 10^{-3} . The low amplitude particles, on the other hand, are hardly affected.

2.4 Random noise mode

It is worth noting that the AC mode requires accurate knowledge of the machine tune and a separate procedure for the horizontal and for the vertical case. An alternative use for the electron lens could be to use the device as a random diffuser acting only on the beam halo. I was already observed that,

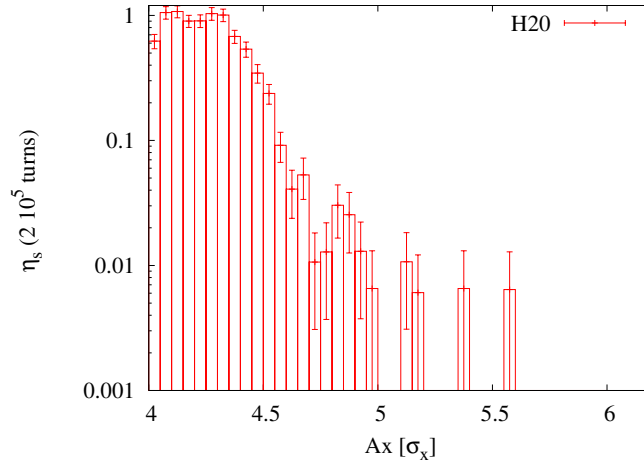


Figure 12: Local scraping inefficiency for the H20 case.

by including a beam current jitter in the DC elens, a mild diffusive effect started to appear. To exploit and maximize this process, the kicks given by the electron lens should include a random component. This can easily be achieved by using a white noise generator to drive the electron lens current. Given the nature of the electron lens, the rms kicks will obviously be larger for high amplitude particles (see the full power kick in Figure 4).

Two different approaches were tested:

- Random mode: the electron beam current was modulated on turn by turn basis by a random multiplier in the range $[0,1]$;
- ON-OFF mode: then electron beam was either reduced to zero (OFF) or at its full power (ON) randomly on a turn-by-turn basis.

The comparison between the two different methods can be appreciated in Figure 13: the global scraping efficiency after $2e5$ turns for the ON-OFF method is about 0.50 ± 0.01 , while for the random method it is only 0.67 ± 0.01 .

The huge advantage of this method is that it is completely uncorrelated with the particle state (both amplitude and tune) and would not require perfect knowledge of the tune or complicated modulation to be performed first for the horizontal and later for the vertical case.

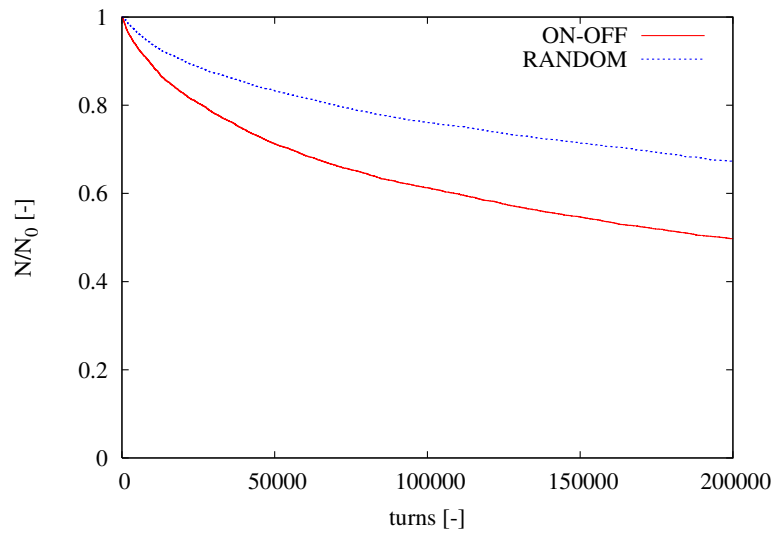


Figure 13: Normalized number of survival particles vs number of turns for the random noise mode. Both ON-OFF and Random method results are presented.

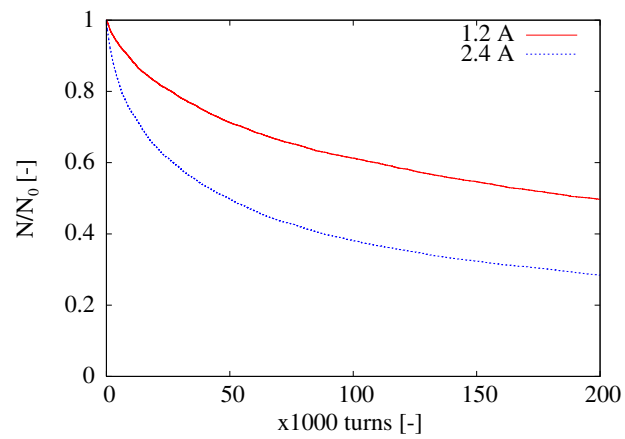


Figure 14: Random effect with double current.

The price to pay for an easier and more robust operation mode is, however, the scraping time. The random ON-OFF about a factor 5 slower than the optimal AC mode: after $2 \cdot 10^5$ turns, only 50% of the particles have been scraped; for this reason longer simulations have been performed. In order to achieve a number of scraper particles comparable with the AC scraping mode, the number of turns has been increased to 10^6 . The number of survival particles versus the turn number is shown in Figure 14. However, being the electron lens kick proportional to the total electron beam current, the scraping efficiency can be easily increased by increasing the beam current. In Figure 14, an electron lens with doubled beam current (2.4 A) is compared with the standard electron lens (1.2 A): in case of enhanced current the global scraping inefficiency is almost halved, reaching a cleaning of more than 70% of the halo particles in 20s.